Corrections to the Calibration of MODIS Aqua Ocean Color Bands Derived From SeaWiFS Data

Gerhard Meister, Bryan A. Franz, Ewa J. Kwiatkowska, and Charles R. McClain

***Abstract*—The National Aeronautics and Space Administration ocean color products of Sea-viewing Wide Field-of-view Sensor (SeaWiFS) and Moderate Resolution Imaging Spectroradiometer (MODIS) Aqua have been reprocessed in 2009. This paper describes the changes to the calibration approach for MODIS Aqua. Due to a significant downward trend in the operational MODIS Aqua water-leaving radiances at 412 nm, the previous calibration approach was no longer sufficient. The new approach uses SeaWiFS water-leaving radiances to adjust the temporal trends of the radiometric calibration of MODIS Aqua bands at 412 and 443 nm. The adjustments to the temporal trends at the beginning of the scan are minor but are significant around nadir and at the end of scan (up to 5% at 412 nm and up to 1% for 443 nm). The remaining five bands (488 to 678 nm) are adjusted with regard to their scan-angle dependence only; no temporal correction is necessary. There is no indication that the sensor polarization sensitivity needs to be modified for MODIS Aqua.**

***Index Terms*—Calibration, image sensors, remote sensing.**

I. Introduction

THERE ARE currently two units of the Moderate Resolution Imaging Spectroradiometer (MODIS) [1] orbiting the earth. The first was launched in December 1999 on National Aeronautics and Space Administration's (NASA) Earth Observing System Terra satellite, and the second was launched on the Aqua satellite in May 2002 [2]. MODIS has 36 spectral bands on four different focal planes. The Ocean Biology Processing Group (OBPG) at NASA uses bands 8–16 (referred to as ocean color bands) with center wavelengths from 412 to 869 nm (see Table I) to produce the standard ocean color data products [3]. The basic ocean color products are water-leaving radiances from bands 8–14 (412 to 678 nm). Bands 15 and 16 (748 and 869 nm) are used to determine the aerosol optical thickness (AOT) and the aerosol type for atmospheric correction [4].

Users obtained more than 6 million files (115 000 GB) of MODIS Aqua data in 2010 from the OBPG website and 3 million files (30 000 GB) of Sea-viewing Wide Field-of-view Sensor (SeaWiFS) data. SeaWiFS [5] is another spaceborne radiometer with similar ocean color bands to MODIS (see Table I). It was launched five years before MODIS Aqua and ceased operation in 2010. Data product consistency between missions is essential if the data sets are to be merged to achieve increased temporal and spatial coverage and long-term seamless time series required for climate research in particular [6]. Product consistency begins with sensor calibration and progresses through the level-2 processing where differences due to viewing geometry and time of day are removed through normalization of the water-leaving radiances and reflectances. From the perspective of data merging to increase spatial coverage, it has been shown [7] that adding MODIS Aqua data to the SeaWiFS global area coverage data increases the daily global coverage at a spatial resolution of 9 km from 16% (SeaWiFS alone) to 29% (SeaWiFS plus MODIS). For the coastal zone, where spatial and temporal scales of variability are much shorter than in the open ocean, coverage from more than one sensor can be essential, e.g., for the detection and tracking of harmful algal blooms, which is a National Oceanic and Atmospheric Administration operational monitoring requirement. Kwiatkowska and McClain [8] consider the influences of differing orbits and equatorial crossing times on global sampling over a day using SeaWiFS, MODIS Aqua, and MODIS Terra for the purposes of examining diurnal variability in chlorophyll concentrations. They show that the three sensors together provide chlorophyll retrievals for up to 6 h (roughly, 9 A.M. to 3 P.M. local time).

The OBPG is trying to achieve a *relative* stability of the radiometric calibration for the MODIS Aqua ocean color data set on the order of $\pm 0.2\%$, which surpasses the official requirements for the MODIS reflective solar bands (bands 1–19 and 26). The MODIS calibration factor m_1 [defined hereinafter, see (2)] can be decomposed into a time (t) independent and a time dependent component $d(t)$

$$m_1(t) = m_1(t = t_0) \cdot d(t)$$
$$d(t = t_0) = 1 \tag{1}$$

where t_0 is, e.g., the time of the first on-orbit solar diffuser measurement. For ocean color, *relative* stability [the accuracy of $d(t)$] is critical for producing climate data records (defined as "a time series of measurements of sufficient length, consistency, and continuity to determine climate variability and change" [9]), whereas the *absolute* calibration uncertainty [the accuracy of $m_1(t = t_0)$] is of lesser importance for the ocean color algorithms because most bands are vicariously calibrated [10], [11]. The MODIS Calibration and Support Team (MCST) provides the calibration trending for all bands of both MODIS

Manuscript received December 3, 2010; revised June 1, 2011; accepted June 11, 2011. Date of publication August 18, 2011; date of current version December 23, 2011.

G. Meister, B. A. Franz, and C. R. McClain are with Ocean Ecology Branch (Code 614.2), Goddard Space Flight Center, National Aeronautics and Space Administration, Greenbelt, MD 20771 USA (e-mail: Gerhard.Meister@nasa.gov).

E. J. Kwiatkowska was with Ocean Biology Processing Group (Code 614.2), Goddard Space Flight Center, Greenbelt, MD 20771 USA. She is now with the European Space Research and Technology Centre, European Space Agency, 2201 Noordwijk, The Netherlands.

Digital Object Identifier 10.1109/TGRS.2011.2160552

TABLE I
MODIS OCEAN COLOR BANDS (8–16), THEIR CENTER WAVELENGTHS λ, AND THE CENTER WAVELENGTHS OF THE CORRESPONDING SEAWIFS BANDS

MODIS band number	8	9	10	11	12	13	14	15	16
MODIS λ[nm]	412	443	488	531	547	667	678	748	869
SeaWiFS λ[nm]	412	445	490	510	555	670		765	865

instruments. For the ocean color bands, they estimated a relative stability on the order of 0.5% for the first three years of the mission [12].

Both MODIS instruments are calibrated using onboard calibrators [13] and lunar irradiances [14]. For MODIS Aqua, these calibration sources have been sufficient to produce high-quality ocean color products [3] up to 2007. For MODIS Terra, this has not been the case [15]. To address this problem, the OBPG developed an on-orbit recharacterization approach for instrument radiometric response using SeaWiFS as a truth field [16]. The cross-calibration method developed for MODIS Terra has now been applied to improve the ocean color products of MODIS Aqua. This paper presents the MODIS Aqua results using the latest MODIS and SeaWiFS calibration improvements, which were applied in the reprocessing of MODIS Aqua. Both the MODIS Aqua and SeaWiFS reprocessings are referred to as "R2009.1"; see the OBPG website (http://oceancolor.gsfc.nasa.gov/WIKI/OCReproc.html) for further details about the reprocessings.

The impact of the cross-calibration corrections is evaluated by analyzing the ocean color products on a global scale. A change in the calibration is treated as a processing configuration change by the OBPG. For each configuration change, the OBPG usually processes a temporal subset of the complete data set and compares it to the data without the configuration change. Each such test is named, e.g., "AT42" is the 42nd temporal test (T) of MODIS Aqua data (A). This paper focuses on the calibration changes of the MODIS Aqua reprocessing R2009.1, so the tests are compared where the only configuration change was the sensor calibration change of interest. (SeaWiFS data are presented in this paper only with the calibration methodology of the SeaWiFS reprocessing R2009.1.) Several configuration changes occurred after the calibration changes were tested that are not directly related to sensor calibration (e.g., ocean color product algorithm changes). These changes are not documented in this paper, and the results presented here do not necessarily contain the exact configuration of the MODIS Aqua reprocessing R2009.1. However, we are not aware of any significant differences with regard to the plots presented in this paper. Rerunning these tests with the final configuration (modifying only the calibration change of interest) would be a significant expense of resources without a relevant gain of knowledge.

The underlying approach of the recharacterization described by *Kwiatkowska et al.* [16] is to derive three separate correction coefficients (one for the radiometric calibration and the other two for the polarization correction) for each sensor element (i.e., each detector and each mirror side). Each coefficient is derived as a function of time and scan angle; see Sections III and IV. The radiometric gain correction is calculated relative to the standard MODIS calibration described in Section II. The impact of applying the correction coefficients is described in Section V-B.

II. STANDARD MODIS CALIBRATION AND CHARACTERIZATION METHODS

The standard MODIS calibration equation [13] uses the calibration coefficient m_1 to describe changes in the radiometric sensitivity of the instrument. The m_1's are used to derive Earth scene reflectance factors ρ_{EV} from the measured counts of the Earth scene (dn_{EV}) with

$$\rho_{EV} \cdot \cos(\theta_{EV}) = m_1 \cdot dn^*_{EV} \cdot d^2_{\mathrm{Earth-Sun}} \tag{2}$$

where ρ_{EV} denotes the top-of-atmosphere (TOA) Earth scene reflectance factors, dn^*_{EV} denotes the temperature- and scan-angle-corrected measured counts after background subtraction, $d_{\mathrm{Earth-Sun}}$ is the distance between Earth and sun in Astronomical Units (AU) at the time of the Earth view measurement, and θ_{EV} is the solar zenith angle. The scan-angle correction is applied by dividing the measured counts dn_{EV} after temperature correction by the *response versus scan* (RVS)

$$dn^*_{EV} = dn_{EV}/RVS(\theta_{\mathrm{AOI}}). \tag{3}$$

The RVS is a function of the angle of incidence (θ_{AOI}) on the MODIS scan mirror, normalized to one at the angle corresponding to the solar diffuser measurement. This means that m_1 is the gain only at the solar diffuser angle; for all other angles, the gain is m_1 divided by the RVS.

The calibration source for determining m_1 on orbit is the solar diffuser. The solar diffuser is viewed at an angle of incidence on the scan mirror of 50.3°, corresponding to frame 979 (each MODIS scan line consists of 1354 frames). The calibration source for determining the RVS is the lunar measurements through the space view port. The moon is viewed at an angle of incidence on the scan mirror of 11.4° [17] (corresponding to frame 22). The radiometric response for all other angles of incidence is modeled, combining the solar diffuser, lunar, and prelaunch characterization measurements at various angles.

MCST has developed a new approach for trending the RVS of bands 13–16. Because the lunar measurements for these bands are mostly saturated [17], the prelaunch RVS was not modified with time. The new approach uses ratios of nonsaturated bands to derive changes in the RVS of bands 13–16 [18]. The new approach was applied before the cross calibration to SeaWiFS was calculated. Its impact on the ocean color products is shown in Section V-A.

The polarization correction for an instrument with polarization sensitivity and an inaccurate radiometric calibration factor is [19]

$$L_m = M_{11}L_t + M_{12}(Q_t \cos 2\alpha + U_t \sin 2\alpha) + M_{13}(-Q_t \sin 2\alpha + U_t \cos 2\alpha) + M_{14}V_t \quad (4)$$

where (L_t, Q_t, U_t, V_t) is the Stokes' vector at the TOA, L_m is the measured radiance, and α is a rotation angle to adjust for different reference frames used in the calculation of Q_t and U_t. M_{11}, M_{12}, M_{13}, and M_{14} are the elements of the first row of the Mueller matrix. (For an instrument without polarization sensitivity, $M_{12} = M_{13} = M_{14} = 0$. For an instrument with an accurate radiometric calibration factor (accurate m_1 and RVS in the case of MODIS), $M_{11} = 1$.) Since V_t is very close to zero at the TOA, M_{14} is an irrelevant parameter for MODIS. The parameters M_{12} and M_{13} were determined prelaunch at scan angles from -45° to $+45^\circ$, for each band, mirror side, and detector [20]. The variations of these parameters with detector were considered suspect and not applied in the ocean color processing [21].

III. Cross-Calibration Method

The cross-calibration method has been described by Kwiatkowska *et al.* [16], so here, we provide only a brief summary. The analysis is performed using a global deep-water ($>$ 1000 m depth) MODIS Aqua data set from one day (approximately 14 orbits) out of every month. The level-3 water-leaving radiances from SeaWiFS (a 15-day composite centered on the day of interest, screened for several criteria, e.g., a maximum AOT at 865 nm of 0.15, chlorophyll concentration of less then 0.15 mg/m^3) are used to predict the TOA radiances as seen by MODIS on that day, using the atmospheric correction approach from Gordon and Wang [22] in reverse mode [10]. The near-infrared (NIR) bands of MODIS are assumed to be sufficiently well calibrated, and no correction is derived for these bands. All components of the Stokes' vector (L_t, Q_t, U_t, V_t) are modeled. This allows not only a retrieval for the radiometric gain parameters M_{11} but also for the polarization parameters M_{12} and M_{13}. The modeled TOA radiances are compared to the radiances measured by MODIS for every scan angle, mirror side, and detector. This means that the Mueller matrix elements M_{11}, M_{12}, and M_{13} can be derived as a function of scan angle, mirror side, and detector. To reduce noise, the scan-angle dependence is modeled by a cubic function for M_{11}, as a linear function for M_{12} and M_{13}. For the radiometric gain correction, this means that (2) effectively becomes

$$\rho_{EV} \cdot \cos(\theta_{EV}) = m_1 \cdot \frac{dn_{EV}}{RVS} \cdot d^2_{\text{Earth-Sun}} \cdot \frac{1}{M_{11}}. \quad (5)$$

Vicarious calibration coefficients [10] using *in situ* data from the Marine Optical Buoy (MOBY [23]) are derived using the TOA radiances after correction with the aforementioned method and are applied before the calculation of the ocean color products.

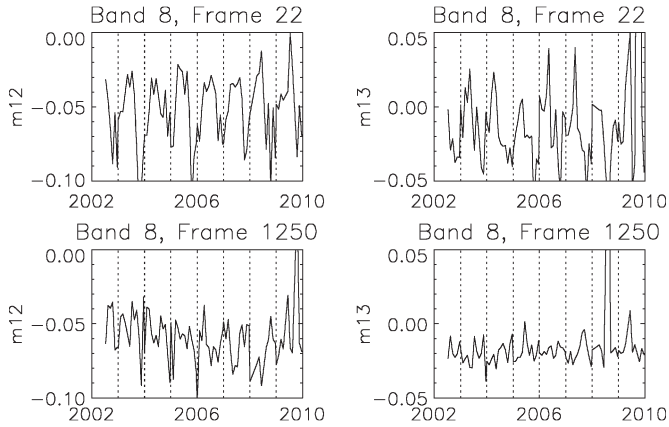

Fig. 1. MODIS Aqua band 8 (mirror side 1, detector 1) polarization coefficients (left) $m_{12} = M_{12}/M_{11}$ and (right) $m_{13} = M_{13}/M_{11}$ as a function of time for two different scan angles: (frame 22, top row) lunar view angle and (frame 1250, bottom row) end of scan. Dashed lines mark yearly intervals to show seasonality of oscillations.

IV. MODIS Aqua Correction Coefficients

A. Polarization Sensitivity

The retrieval of the Mueller matrix elements is repeated for one day in every month of the mission. This results in a time series as shown in Fig. 1 for band 8.

The polarization coefficients M_{12} for MODIS Terra changed remarkably over the mission, by more than 0.3 for band 8 [16]. For MODIS Aqua, there is no detectable long-term trend in Fig. 1. There is a significant seasonal oscillation which is much stronger than what was found for MODIS Terra by Kwiatkowska *et al.* [16]. The reason for this oscillation is not yet understood. It has significantly increased in a reanalysis in 2010 of the MODIS Terra data. For the reanalysis, the OBPG switched to a new set of aerosol models for the atmospheric correction [4], but it is not clear if this is the reason for the increased oscillation.

Comparing the two scan angles in Fig. 1, it can be seen that the seasonal oscillation is larger at the beginning of the scan than at the end of the scan, for both M_{12} and M_{13}. This is probably due to the fact that the degree of polarization of the TOA radiance, defined as

$$d_p = \frac{\sqrt{Q_t^2 + U_t^2}}{L_t} \quad (6)$$

is much lower (by about 50%) at the beginning of the scan; see Fig. 2. Therefore, it is very difficult to retrieve an accurate polarization sensitivity at the beginning of the scan with (4). The seasonal oscillation most likely is an artifact in the analysis, because there is no plausible theory why the polarization sensitivity of MODIS could have a seasonal oscillation. Since there is no indication that there is a long-term trend, no correction is applied to the prelaunch polarization coefficients. It could be argued that, at the end of the scan, M_{12} shows evidence of a decrease throughout the mission and a rebound in 2010, but the effect is smaller than the seasonal oscillation. It was decided to apply the polarization corrections derived from prelaunch measurements for reprocessing R2009.1, not the polarization coefficients derived from the cross calibration. This was done

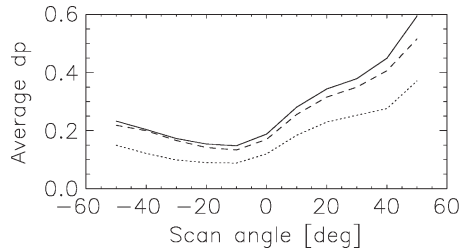

Fig. 2. Average degree of polarization d_p for an orbit over the Pacific in August 2002 (same as shown in Fig. 9(d), [21] by Meister *et al.*) as a function of scan angle. The current polarization correction algorithm calculates the Q and U components of the Stokes' vector only for Rayleigh scattering and glint, not for aerosol scattering. (Solid line) 547 nm. (Dashed line) 412 nm. (Dotted line) 869 nm.

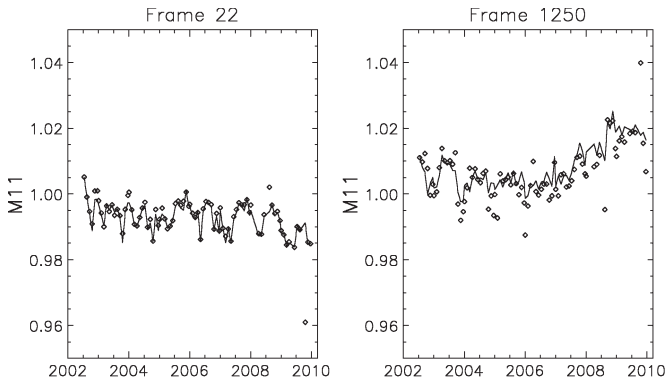

Fig. 3. MODIS Aqua band 8 (mirror side 1, detector 1) M_{11} retrievals (solid line) with prelaunch polarization sensitivities and (diamonds) with polarization sensitivities from the optimization. M_{11} is defined in (4) and represents the ratio of the original over the corrected TOA radiance.

for all bands; the M_{12} of the other bands retrieved from the cross-calibration analysis shows less temporal variation than those of band 8.

B. Radiometric Gain Sensitivity

The retrieval of the Mueller matrix elements was repeated, this time setting the polarization sensitivities M_{12} and M_{13} to their prelaunch value. A comparison of the new M_{11} and the previous ones (where M_{11}, M_{12}, and M_{13} were retrieved simultaneously) is shown in Fig. 3. It can be seen that, at the beginning of scan (frame 22), the agreement between both sets of M_{11} is excellent, except for a few outliers. At the end of scan (frame 1250), there is considerably more scatter, but the long-term trends are very similar for both curves. This shows that the individual M_{11} retrievals are dependent on the polarization sensitivity to a certain extent. However, in the case of MODIS Aqua, the impact on the retrieval of secular correction trends is negligible.

The M_{11} is shown at four scan angles in Fig. 4 for band 8. The results are smoothed over time using fifth-order polynomials before they are applied in the processing of ocean color products. For example, at the end of 2009, Fig. 4 suggests that the TOA radiances of band 8 around frame 500 need to be increased by 5% relative to their value at the beginning of the mission.

Fig. 5 shows the smoothed results for the M_{11} coefficients for bands 9–14 as a function of frame (or view angle). The smoothed M_{11} coefficients are applied as corrections. It can be

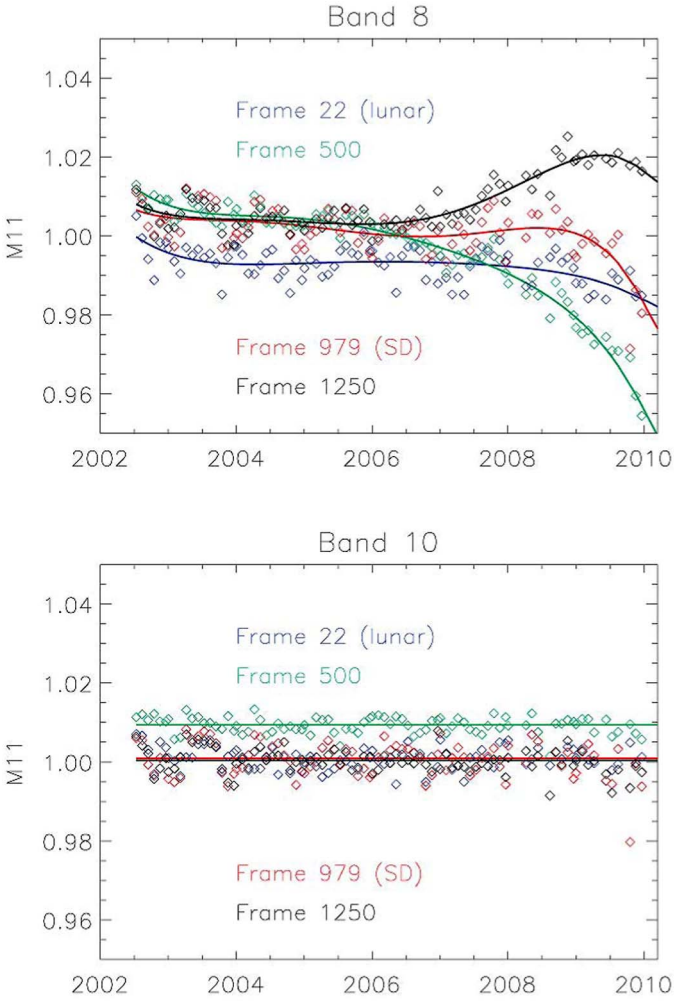

Fig. 4. Mueller matrix elements M_{11} for (left) band 8 and (right) band 10, for mirror side 1 and detector 1, at four different view angles (lunar view angle, close to nadir, solar diffuser, and close to end of scan). M_{11} is defined in (4) and represents the ratio of the original over the corrected TOA radiance. Diamonds show the result of the cross-calibration analysis for each individual day. Solid lines show a fit of a fifth-degree polynomial as a function of time for band 8, a temporal average for band 10.

seen that the corrections required for band 8 are much larger than for the other bands. The corrections for band 9 are usually less than 1%. For bands 10–14, the corrections are so small that it was decided to average the M_{11} coefficients over time but to keep the scan-angle dependence. Therefore, only one line is shown for these bands in Fig. 5. The retrieved M_{11} is shown for band 10 in Fig. 4. It can be seen that there is no recognizable trend. The standard deviation of the ratio of the retrieved M_{11} to the fitted M_{11} for band 10 is comparable to the standard deviations for bands 8 and 9; see Table II. For longer wavelengths, the standard deviations decrease. The standard deviations are lowest for frame 500 (near nadir). This could be related to the fact that the quality of ocean color retrievals increases when the air mass decreases. The standard deviations are highest for frame 1250 (end of scan). This could be a combination of the effects of a high air mass and a higher degree of polarization of the TOA radiance (see Fig. 2 previously mentioned).

Note that the cross-calibration method does not provide corrections for the NIR bands (MODIS Aqua bands 15 and 16).

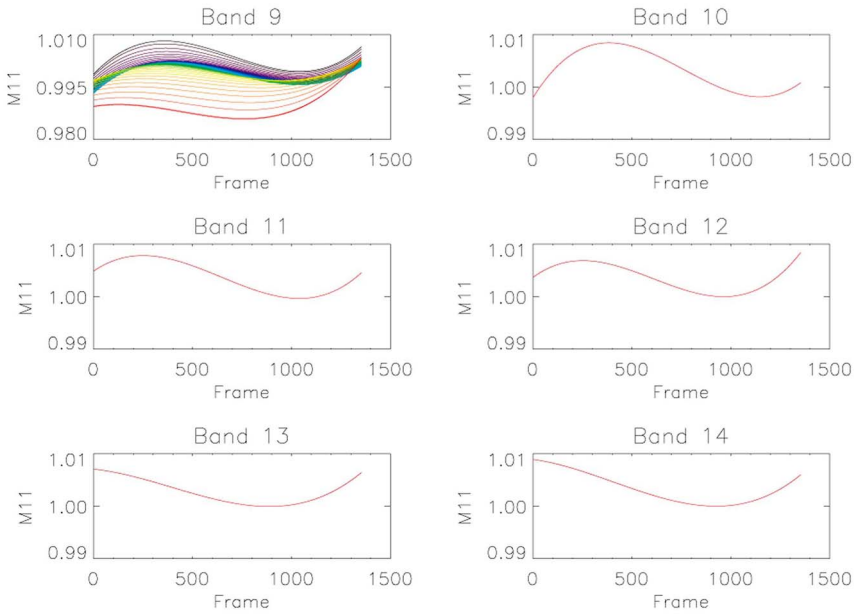

Fig. 5. Correction to the MODIS calibration coefficients for bands 9–14 as a function of frame. The frame is proportional to the view angle, frame $= 0$ corresponds to the beginning of the scan (view angle of $-55°$), and frame $= 1353$ corresponds to the end of the scan (view angle of $+55°$). For band 9, color indicates time using a rainbow scale: Black/blue is for the beginning of the mission (starting in 2002), and red is for the beginning of 2010. Note that the ordinate for band 9 is different from the other bands.

TABLE II
STANDARD DEVIATIONS FOR RATIO OF (DIAMONDS IN FIG. 4) RETRIEVED M_{11} OVER (SOLID LINE IN FIG. 4) TEMPORALLY FITTED M_{11} FOR FOUR DIFFERENT FRAMES (OR SCAN ANGLES) AND FOR DIFFERENT BANDS. THERE ARE 85 M_{11} FOR EACH SCAN ANGLE

Frame	22	500	989	1250
Band 8 stdev [%]	0.37	0.24	0.42	0.29
Band 9 stdev [%]	0.29	0.21	0.39	0.29
Band 10 stdev [%]	0.29	0.21	0.41	0.30
Band 14 stdev [%]	0.20	0.19	0.35	0.23

The fact that no temporal correction is required for the bands from 488 to 678 nm increases our confidence in the assumption that the NIR bands (at 748 and 869 nm) do not require a temporal adjustment either.

The corrections are needed for the operational processing of MODIS Aqua. This is a challenge, because the cross calibration only provides correction coefficients for past time periods. The initial attempt described by Meister *et al.* [24] (a linear extrapolation) to extrapolate the correction for bands 8 and 9 into the future was not successful, particularly for band 8. An approach more likely to succeed is to use the most recent value to process the current data, with monthly checks to see if an update is needed. Unfortunately, since temporal fitting is an important part of the data analysis, the most recent corrections will always have the largest uncertainties.

V. IMPACT ON MODIS AQUA OCEAN COLOR PRODUCTS

A. Impact of NIR RVS Trending Only

The MODIS Aqua normalized fluorescence line height product (nFLH) [25] is extremely sensitive to the difference of bands 13 and 14 (667 and 678 nm, respectively). The previous operational products showed a much stronger decrease in the band 14 remote sensing reflectance than for band 13; see Fig. 6. This lead to a decrease with time of the nFLH product of about 30%. The new lunar trending approach for bands 13–16 by MCST yielded very consistent temporal trends for the remote sensing reflectances of bands 13 and 14 (see Fig. 6), which removed the trend in the nFLH product.

An important part of the ocean color processing is the atmospheric correction, particularly the estimation of the impact of the aerosol type. The aerosol type is used to extrapolate the AOT at the wavelengths where it is measured (748 and 869 nm for MODIS Aqua) to the shorter wavelengths where the water-leaving radiances are measured. Angstrom coefficients $\alpha(\lambda_1)$ define the wavelength dependence of the AOT for a given aerosol type. They are dimensionless and defined for MODIS Aqua ocean color products as

$$\frac{\tau_a(\lambda_1)}{\tau_a(\lambda_2)} = \left(\frac{\lambda_1}{\lambda_2}\right)^{-\alpha(\lambda_1)} \tag{7}$$

where $\lambda_2 = 869$ nm for MODIS Aqua ocean color products. Note that, for the reprocessing 2009, λ_1 was changed from 531 to 443 nm to improve consistency with AERONET [26] products.

The new lunar calibration approach reduces a long-term increase in the global Angstrom coefficients; see Fig. 7. The increase over the time period analyzed (mid-2002 to mid-2009) has been reduced from 0.09 to 0.06 (with an average Angstrom of about 0.61 and 0.62, respectively). It is not clear whether this is an improvement or not. The SeaWiFS data show an even larger increase over the same time period. However, the SeaWiFS orbit has been changing significantly since 2007, which could affect the Angstrom time series (e.g., due to a change in undetected glint; the OBPG atmospheric correction

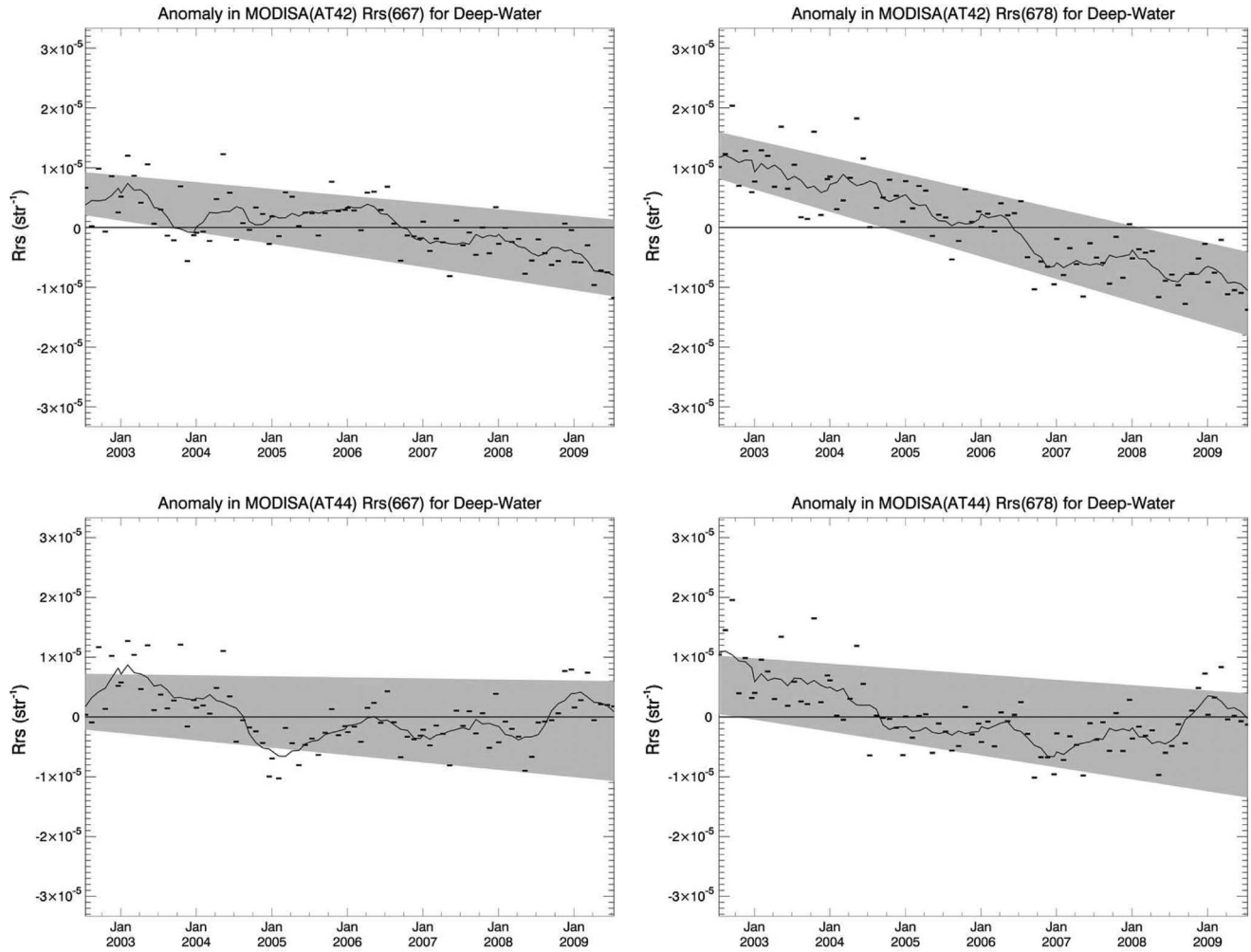

Fig. 6. Temporal anomaly of (left) $Rrs(667)$ and (right) $Rrs(678)$ (top) without and (bottom) with the application of NIR RVS trending. The anomaly plots (Figs. 6–8) were calculated by removing the seasonal cycle from the global average of the data for the respective area (deep water in this case). The error bars indicate the standard deviation around each average (from spatial averaging); the solid line shows the smoothed anomaly. The gray area indicates the range of linear trends; see Franz *et al.* [15] for further details.

process treats uncorrected residual glint contamination as aerosol radiance).

B. Impact of NIR RVS Trending and Cross-Calibration Combined

The impact of the cross calibration on the MODIS Aqua remote sensing reflectance at 412 nm [$Rrs(412)$] for the deep-water region is shown in Fig. 8. The large drop after 2007 of about 15% has been removed. Additionally, a difference at the beginning of the mission of about 5% has been eliminated as well. Over the whole mission, the Rrs at 412 nm in deep water after cross calibration increases by about 5%, in good agreement with SeaWiFS. It should be noted that good agreement is expected. Good agreement of the ocean color products demonstrates the consistency of our approach, not its accuracy.

Note that the gray line in Fig. 8 shows the anomaly before cross calibration but with the NIR RVS trending. The NIR RVS trending actually increased the drop in the remote sensing reflectance Rrs 412 nm anomaly after 2007 from approximately 8% to 15%, most likely due to the change in aerosol characteristics shown in Fig. 7.

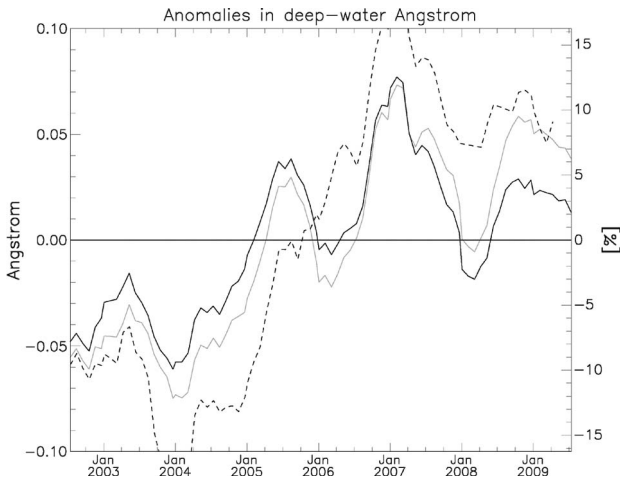

Fig. 7. (Smoothed) Angstrom temporal anomaly (black/gray) with/without application of NIR RVS trending. Both data sets (AT42 and AT44) were calculated with the application of the cross-calibration corrections. Dashed line is for SeaWiFS (ST73).

The impact of the cross calibration on the 443 nm anomaly is similar to that of 412 nm but of a much smaller magnitude. A mission long decrease of about 5% has become an increase

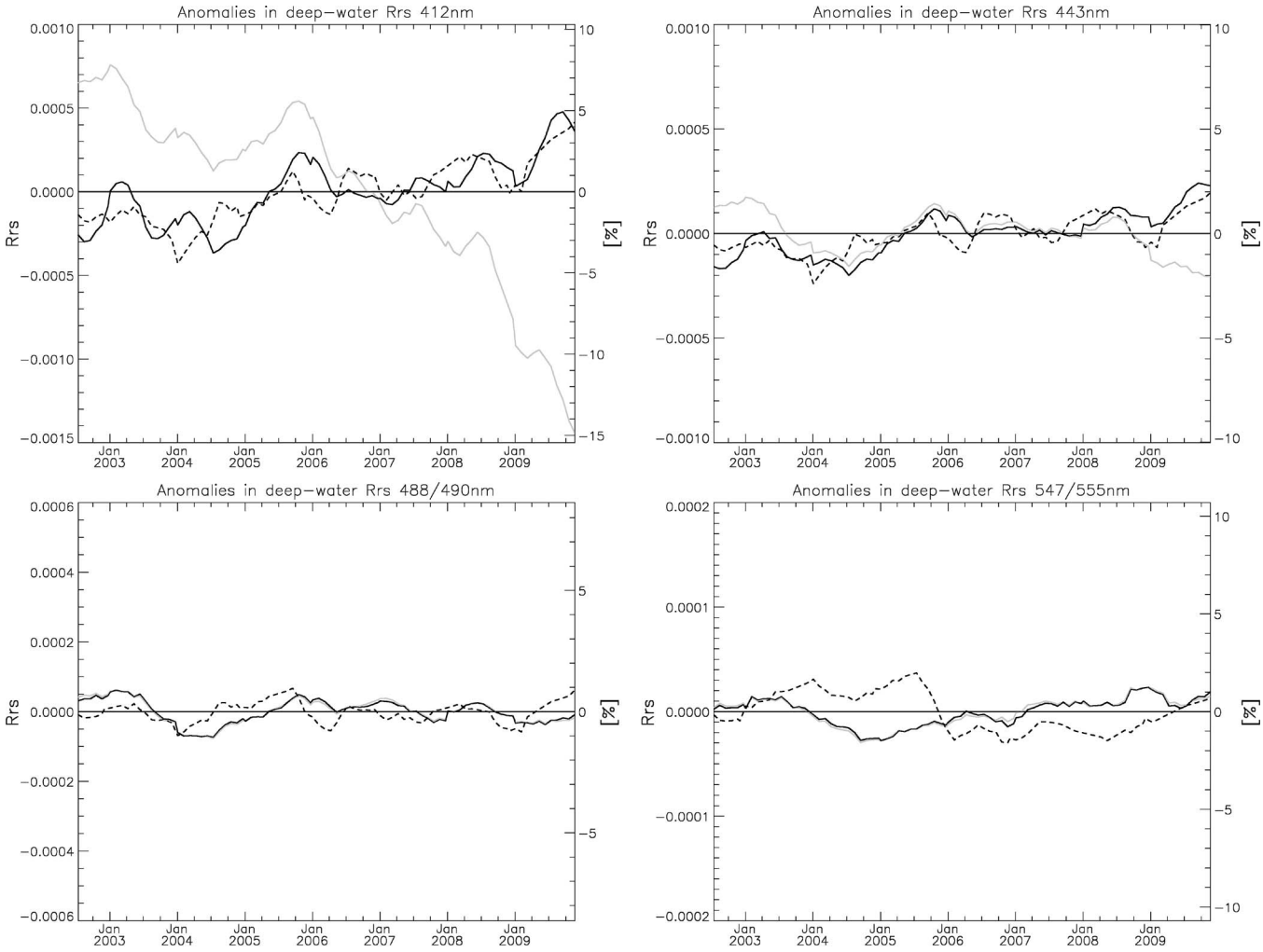

Fig. 8. (Smoothed) Temporal anomaly of Rrs at 412, 443, 488(490), and 547(555) nm for deep water. Numbers in parentheses indicate SeaWiFS center wavelengths (if different from MODIS). Solid black line shows anomaly after cross calibration (test AT51), gray line before cross calibration (test AT47), and dashed line for SeaWiFS operational products (ST76, 2009 reprocessing).

of about 3%, in good agreement with the SeaWiFS trends. At 488 and 547 nm, the trends over the whole mission are within $\pm 1\%$ for both MODIS Aqua and SeaWiFS. (The gray and black lines are almost indistinguishable in Fig. 8 for 488 and 547 nm because temporally dependent corrections were only applied to the bands at 412 and 443 nm.)

The scan-angle dependence of the remote sensing reflectance of all bands has been improved, mostly due to the application of the M_{11} cross-calibration coefficients (the NIR RVS trending only had a minor impact on the scan-angle dependence, except for bands 13 and 14). Improvements were achieved for all bands; examples are shown in Fig. 9 for the end of the mission, the most challenging period. For day 289 of 2009, the water-leaving radiances at 412 nm varied by more than 20% as a function of scan angle; application of the cross calibration reduced this effect to less than 5%. For 443 nm, the variation was reduced from about 5% to about 2%.

Bands 13 and 14 still show a residual scan-angle dependence in the later part of the mission. The water-leaving radiances of these two bands are extremely sensitive to calibration errors, because the water-leaving radiance is usually less than 1% of the TOA radiance at these wavelengths. This is why the relatively small cross-calibration correction (see Fig. 5, less than 1%) changes the scan-angle variation of the band 14 Rrs in Fig. 9 from about 50% to about 10%. This is also the reason for the elevated noise for 678 nm in Fig. 9 compared to the results at 412 and 443 nm; at the later two wavelengths, the water-leaving radiance is about 10% to 15% of the TOA radiance.

According to our analysis tools, striping became a noticeable issue for the shorter wavelengths of MODIS Aqua after 2007. (MODIS has ten detectors per scan line, and small calibration errors of the detectors relative to each other are easily identified in the ocean color product images as striping; on the other hand, a calibration error common to all detectors will not lead to striping.) Fig. 9 also shows that the cross calibration has improved the striping in the images. This is indicated by the fact that the different lines are much closer together after the cross calibration. For day 289 of 2009, the water-leaving radiances at 412 nm varied by almost 10% from detector to detector and by up to 5% between mirror sides (averaging over detectors). The cross calibration almost completely removed these differences for wavelengths below 600 nm. However, striping is still present in the red bands.

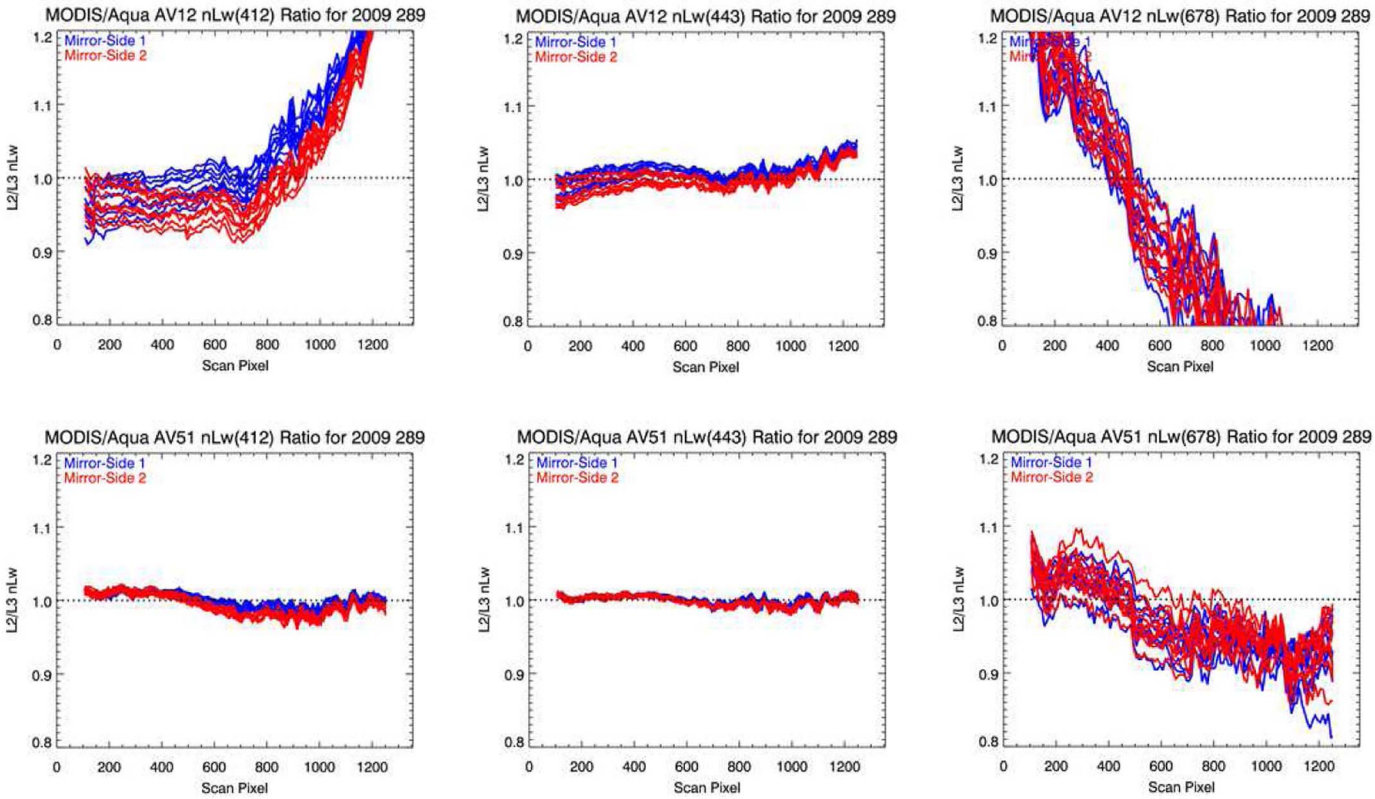

Fig. 9. Residual scan-angle dependence of MODIS Aqua level-2 products (top, AV12) before and (bottom, AV51) after cross calibration. Columns from left to right show nLw at 412, 443, and 678 nm. Each line represents the globally averaged mean ratio of L2 data for day 289 of 2008 at the respective scan pixel (or frame) of one of the ten MODIS detectors to the corresponding L3 bin (seven-day average, 9 km × 9 km spatial resolution). Blue and red are for mirror sides 1 and 2, respectively. See Franz *et al.* [15] for further details. The OBPG changed its product suite from water-leaving radiance (nLw) to remote sensing reflectance (Rrs) for the 2010 reprocessing; the two quantities are proportional to each other; however, the analysis tool for the scan-angle dependence has not been updated yet.

VI. Conclusion

The traditional calibration approach of using lunar and solar diffuser measurements was sufficient for MODIS Aqua from 2002 to 2007. Trends in the remote sensing reflectances at 412 and 443 nm started to deviate from their historic pattern in 2008. These deviations have been shown by an analysis of only MODIS Aqua data and by a comparison of MODIS Aqua data to equivalent SeaWiFS products (see Fig. 8). The OBPG decided to use the SeaWiFS ocean color products to adjust the MODIS Aqua calibration using the same methodology as used for MODIS Terra [16]. Compared to MODIS Terra, the adjustments for MODIS Aqua are much smaller for the radiometric gains (maximum of about 5% for MODIS Aqua versus a maximum adjustment of about 15% for MODIS Terra), and an adjustment for the polarization sensitivity of MODIS Aqua is not needed (adjustment of up to about 30% needed for MODIS Terra). Also, a temporal adjustment is only needed for the two shortest wavelengths of MODIS Aqua (412 and 443 nm); the bands from 488 to 678 nm require only a minor time-independent scan-angle correction of about 1%. The cross calibration of MODIS Aqua to SeaWiFS has resulted in ocean color products that are very consistent for the two sensors. This is desirable mainly for two reasons.

1) The ocean color products of SeaWiFS are recognized in the community for their excellent temporal quality, which is due to a superior radiometric calibration based on lunar measurements [27]. By modifying the MODIS Aqua temporal calibration trends for bands 8 and 9, the SeaWiFS temporal calibration accuracy has been transferred to MODIS Aqua.
2) The consistency of the temporal trends of the two sensors allows a meaningful merger of the two data sets, e.g., for the chlorophyll-a concentration product. It is likely that merging nonocean products would also benefit [28], [29].

However, the cross-calibration approach also has disadvantages.

1) If there is an erroneous trend in the SeaWiFS ocean color products, it will be imposed onto the MODIS Aqua ocean color products.
2) The SeaWiFS sensor has ceased operation in December 2010. The cross-calibration approach needs to be replaced by another method to continue the MODIS Aqua climate data record. Although it may be feasible to use climatology data instead of SeaWiFS L3 data, this may prevent MODIS Aqua from detecting global change of the ocean color products, which is one of its main purposes. No approach has been chosen so far, but it is likely that a solution will involve relying on the lunar data (measured at the beginning of the scan, which have been reliable so far and are expected to be reliable in the future) and a cross calibration with climatologies to adjust the calibration of the remaining scan angles *relative* to the

lunar angle. Another source of truth data could be well calibrated *in situ* water-leaving radiance measurements (e.g., from MOBY [23]). However, noise in the matchups (about 1%, see [10, Table II]) and the infrequency of matchups that pass quality control (one to two per month for the MOBY site for MODIS Aqua) are not sufficient to derive time- and scan-angle-dependent correction coefficients. For the vicarious calibration procedure used by the OBPG, it takes several years of data to acquire one stable vicarious gain coefficient per band [10].

3) SeaWiFS has only one band in red (670 nm), whereas MODIS Aqua has two (667 and 678 nm). Using one SeaWiFS band to adjust the temporal trends in both MODIS Aqua red bands will always result in identical temporal trends for the two MODIS Aqua bands, thereby making it impossible to detect any global change in the nFLH product, which is calculated using the difference of the two bands. Fortunately, at the moment, only the shorter wavelength bands (412 and 443 nm) require a temporal adjustment.
4) The calibration adjustments to MODIS Aqua can only be calculated for data from the past. An extrapolation of the past adjustments into the present and near future is necessary for real-time processing. This adds uncertainty and may result in the need to frequently reprocess the recent data (e.g., every six months).

ACKNOWLEDGMENT

The authors would like to thank the members of the MODIS Calibration and Support Team, particularly J. Sun and J. Xiong, and two anonymous reviewers for their comments.

REFERENCES

[1] W. L. Barnes, T. S. Pagano, and V. V. Salomonson, "Prelaunch characteristics of the Moderate Resolution Imaging Spectroradiometer (MODIS) on EOS-AM1," *IEEE Trans. Geosci. Remote Sens.*, vol. 36, no. 4, pp. 1088–1100, Jul. 1998.

[2] C. L. Parkinson, "Aqua: An earth-observing satellite mission to examine water and other climate variables," *IEEE Trans. Geosci. Remote Sens.*, vol. 41, no. 2, pp. 173–183, Feb. 2003.

[3] B. A. Franz, P. J. Werdell, G. Meister, S. W. Bailey, R. E. Eplee, G. C. Feldman, E. Kwiatkowska, C. R. McClain, F. S. Patt, and D. Thomas, "The continuity of ocean color measurements from SeaWiFS to MODIS," *Proc. SPIE*, vol. 5882, p. 588 20W, 2005.

[4] Z. Ahmad, B. A. Franz, C. R. McClain, E. J. Kwiatkowska, J. Werdell, E. P. Shettle, and B. N. Holben, "New aerosol models for the retrieval of aerosol optical thickness and normalized water-leaving radiances for the SeaWiFS and MODIS sensors over coastal regions and open oceans," *Appl. Opt.*, vol. 49, no. 29, pp. 5545–5560, Oct. 2010.

[5] C. R. McClain, G. C. Feldman, and S. B. Hooker, "An overview of the SeaWiFS project and strategies for producing a climate research quality global ocean bio-optical time series," *Deep-Sea Res. II*, vol. 51, no. 1–3, pp. 5–42, Jan./Feb. 2004.

[6] C. R. McClain, S. B. Hooker, G. C. Feldman, and P. Bontempi, "Satellite data for ocean biology, biogeochemistry, and climate research," *EOS Trans. AGU*, vol. 87, no. 34, pp. 337–343, 2006.

[7] "Ocean-color data merging," Dartmouth, NS, Canada, IOCCG Rep. 6, 2007.

[8] E. J. Kwiatkowska and C. R. McClain, "Capabilities for extracting phytoplankton diurnal variability using ocean color data from SeaWiFS, MODIS-Terra, and MODIS-Aqua," *Int. J. Remote Sens.*, vol. 30, no. 24, pp. 6441–6459, 2009.

[9] "Climate data records from environmental satellites: Interim report," National Academy Press, Washington, DC, 2004.

[10] B. A. Franz, S. W. Bailey, P. J. Werdell, and C. R. McClain, "Sensor-independent approach to the vicarious calibration of satellite ocean color radiometry," *Appl. Opt.*, vol. 46, no. 22, pp. 5068–5082, Aug. 2007.

[11] R. A. Barnes, R. E. Eplee, Jr., G. M. Schmidt, F. S. Patt, and C. R. McClain, "Calibration of SeaWiFS. I. Direct techniques," *Appl. Opt.*, vol. 40, no. 36, pp. 6682–6700, Dec. 2001.

[12] J. A. Esposito, X. Xiong, A. Wu, J. Sun, and W. L. Barnes, "MODIS reflective solar bands uncertainty analysis," *Proc. SPIE*, vol. 5542, pp. 448–458, 2004.

[13] X. Xiong, J. Sun, X. Xie, W. L. Barnes, and V. V. Salomonson, "On-orbit calibration and performance of Aqua MODIS reflective solar bands," *IEEE Trans. Geosci. Remote Sens.*, vol. 48, no. 1, pp. 535–546, Jan. 2010.

[14] J. Sun, X. Xiong, W. Barnes, and B. Guenther, "MODIS reflective solar bands on-orbit lunar calibration," *IEEE Trans. Geosci. Remote Sens.*, vol. 45, no. 7, pp. 2383–2393, Jul. 2007.

[15] B. A. Franz, E. J. Kwiatkowska, G. Meister, and C. R. McClain, "Moderate Resolution Imaging Spectroradiometer on Terra: Limitations for ocean color applications," *J. Appl. Remote Sens.*, vol. 2, p. 023 525, Jun. 2008.

[16] E. J. Kwiatkowska, B. A. Franz, G. Meister, C. R. McClain, and X. Xiong, "Cross calibration of ocean-color bands from Moderate-Resolution Imaging Spectroradiometer on Terra platform," *Appl. Opt.*, vol. 47, no. 36, pp. 6796–6810, Dec. 2008.

[17] R. E. Eplee, X. Xiong, J.-Q. Sun, G. Meister, and C. R. McClain, "The cross calibration of SeaWiFS and MODIS using on-orbit observations of the moon," in *Proc. SPIE—Earth Observing Systems XIV*, J. J. Butler and J. Xiong, Eds., 2009, vol. 7452, p. 745 235.

[18] B. N. Wenny, J.-Q. Sun, X. Xiong, A. Wu, H. Chen, A. Angal, T. Choi, N. Chen, S. Madhavan, X. Geng, J. Kuyper, and L. Tan, "MODIS calibration algorithm improvements developed for collection 6 level-1b," in *Proc. SPIE—Earth Observing Systems XV*, J. J. Butler, J. Xiong, and X. Gu, Eds., 2010, vol. 7807, p. 780 71F.

[19] H. R. Gordon, T. Du, and T. Zhang, "Atmospheric correction of ocean color sensors: Analysis of the effects of residual instrument polarization sensitivity," *Appl. Opt.*, vol. 36, no. 27, pp. 6938–6948, Sep. 1997.

[20] J. Sun and X. Xiong, "MODIS polarization sensitivity analysis," *IEEE Trans. Geosci. Remote Sens.*, vol. 45, no. 9, pp. 2875–2885, Sep. 2007.

[21] G. Meister, E. J. Kwiatkowska, B. A. Franz, F. S. Patt, G. C. Feldman, and C. R. McClain, "Moderate-Resolution Imaging Spectroradiometer ocean color polarization correction," *Appl. Opt.*, vol. 44, no. 26, pp. 5524–5535, Sep. 2005.

[22] H. R. Gordon and M. Wang, "Retrieval of water-leaving radiance and aerosol optical thickness over the oceans with SeaWiFS: A preliminary algorithm," *Appl. Opt.*, vol. 33, no. 3, pp. 443–452, Jan. 1994.

[23] S. W. Brown, S. J. Flora, M. E. Feinholz, M. A. Yarbrough, T. Houlihan, D. Peters, Y. S. Kim, J. L. Mueller, B. C. Johnson, and D. K. Clark, "The Marine Optical BuoY (MOBY) radiometric calibration and uncertainty budget for ocean color satellite sensor vicarious calibration," in *Proc. SPIE—Sensors, Systems, and Next-Generation Satellites*, Sep. 2007, vol. 6744, p. 674 41M.

[24] G. Meister, B. A. Franz, E. J. Kwiatkowska, and C. R. McClain, "Corrections to the calibration of MODIS Aqua ocean color bands derived from SeaWiFS data," in *Proc. IEEE IGARSS*, 2010, pp. 3688–3691.

[25] M. J. Behrenfeld, T. K. Westenberry, E. S. Boss, R. T. O'Malley, D. A. Siegel, J. D. Wiggert, B. A. Franz, C. R. McClain, G. C. Feldman, S. C. Doney, J. K. Moore, G. Dall'Omo, A. J. Milligan, I. Lima, and N. Mahowald, "Satellite-detected fluorescence reveals global physiology of ocean phytoplankton," *Biogeosciences*, vol. 6, no. 5, pp. 779–794, Jan. 2009.

[26] B. N. Holben, T. F. Eck, I. Slutzker, D. Tanré, J. P. Buis, A. Setzer, E. Vermote, J. A. Reagan, Y. J. Kaufman, T. Nakajima, F. Lavenu, I. Jankowiak, and A. Smirnov, "AERONET—A federated instrument network and data archive for aerosol characterization," *Remote Sens. Environ.*, vol. 66, no. 1, pp. 1–16, Oct. 1998.

[27] M. J. Behrenfeld, R. T. O'Malley, D. A. Siegel, C. R. McClain, J. L. Sarmiento, G. C. Feldman, P. G. Falkowski, E. S. Boss, and A. J. Milligan, "Climate-driven trends in contemporary ocean productivity," *Nature*, vol. 444, no. 7120, pp. 752–755, Dec. 2006.

[28] M. Jeong, N. C. Hsu, E. J. Kwiatkowska, B. A. Franz, G. Meister, and C. E. Salustro, "Impacts of cross-platform vicarious calibration on the deep blue aerosol retrievals for Moderate Resolution Imaging Spectroradiometer aboard Terra," *IEEE Trans. Geosci. Remote Sens.*, vol. 49, no. 12, pp. 4877–4888, Dec. 2011. [Online]. Available: http://ieeexplore.ieee.org/xpls/abs_all.jsp?arnumber=5928405

[29] V. Zubko, G. G. Leptoukh, and A. Gopalan, "Study of data-merging and interpolation methods for use in an interactive online analysis system: MODIS Terra and Aqua daily aerosol case," *IEEE Trans. Geosci. Remote Sens.*, vol. 48, no. 12, pp. 4219–4235, Dec. 2010.

Gerhard Meister received the Diploma and Ph.D. degrees in physics from the University of Hamburg, Hamburg, Germany, in 1996 and 2000, respectively.

From 2000 to 2010, he was with Futuretech Corporation in collaboration with the Ocean Biology Processing Group, Goddard Space Flight Center, National Aeronautics and Space Administration (NASA), Greenbelt, MD. Since 2010, he has been a Member with the Ocean Ecology Branch (Code 614.2), NASA. His main focus is the calibration and characterization of satellite-based ocean color sensors such as Moderate Resolution Imaging Spectroradiometer, Sea-viewing Wide Field-of-view Sensor, and Visible–Infrared Imaging Radiometer Suite.

Bryan A. Franz received the B.S. degree in aerospace engineering from the University of Maryland, College Park, in 1988 and the M.S. degree in computer science from Johns Hopkins University, Baltimore, MD, in 1998.

He is currently a Scientist with the Ocean Ecology Branch (Code 614.2), Goddard Space Flight Center, National Aeronautics and Space Administration, Greenbelt, MD, where he leads the ocean color reprocessing efforts for Moderate Resolution Imaging Spectroradiometer (MODIS), Sea-viewing Wide Field-of-view Sensor, and other sensors within the Ocean Biology Processing Group. He also serves as the Ocean Discipline Lead for the MODIS Science Team. His work focuses on atmospheric correction and bio-optical algorithms, calibration, and validation for satellite remote sensing of marine environments, with emphasis on consistent processing methods across multiple missions.

Ewa J. Kwiatkowska received the M.Sc. degree from the Department of Applied Mathematics, Warsaw University of Technology, Warsaw, Poland, and the M.Phil. and Ph.D. degrees from the Department of Computing, University of Bradford, Bradford, U.K.

She was with the Japanese Space Agency's Earth Observation Research Center for two years working on ocean color and temperature data. Subsequently, she moved to the United States and was with the Goddard Space Flight Center, National Aeronautics and Space Administration, Greenbelt, MD, where she gained her experience in calibration, validation, and algorithm development for ocean color satellite instruments. She is currently with the Research and Technology Centre, European Space Agency, Noordwijk, The Netherlands. Her background is in applied mathematics and computer science with accompanying expertise in calibration, validation, and algorithm development for optical satellite missions and ocean color, in particular.

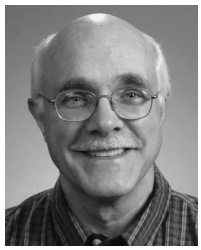

Charles R. McClain received the B.A. degree in physics from William Jewell College, Liberty, MO, in 1970 and the Ph.D. degree in marine science from North Carolina State University, Raleigh, in 1976.

He has held leadership positions associated with the Coastal Zone Color Scanner, Sea-viewing Wide Field-of-view Sensor, the Moderate Resolution Imaging Spectroradiometer, the Sensor Intercomparison and Merger for Biological and Interdisciplinary Oceanic Studies, the National Polar-orbiting Operational Environmental Satellite System Visible–Infrared Imaging Radiometer Suite, and the Aerosol, Cloud, and Ecology programs. He is currently the Leader with the Ocean Ecology Branch (Code 614.2), Goddard Space Flight Center, National Aeronautics and Space Administration, Greenbelt, MD. For over 30 years, his research has focused on the application of satellite ocean color data in studying the linkages between biological and physical processes and the marine carbon cycle.